

5 Atmospheres of Jovian Planets

Nancy Chanover

Astronomy Department, New Mexico State University, Las Cruces,
NM, USA

1	<i>Introduction</i>	224
2	<i>Atmospheric Composition and Structure</i>	227
2.1	Cloud Locations	228
2.1.1	Limitations of Remote Sensing	231
2.2	In Situ Measurements	233
3	<i>Atmospheric Dynamics</i>	234
3.1	Winds	235
3.1.1	Observational Evidence for Seasonal Changes on Uranus and Neptune	236
3.2	Storm Features	239
3.2.1	Jupiter	239
3.2.2	Saturn	241
3.2.3	Uranus and Neptune	243
4	<i>Atmospheric Chemistry</i>	244
4.1	Energy Balance	245
4.2	Case Study: Shoemaker-Levy 9 Impacts on Jupiter	245
5	<i>Future Directions</i>	246
5.1	Unanswered Questions	246
5.2	Future Missions to the Outer Solar System	246
5.3	Links to Exoplanets	248
	<i>Acknowledgments</i>	248
	<i>References</i>	248

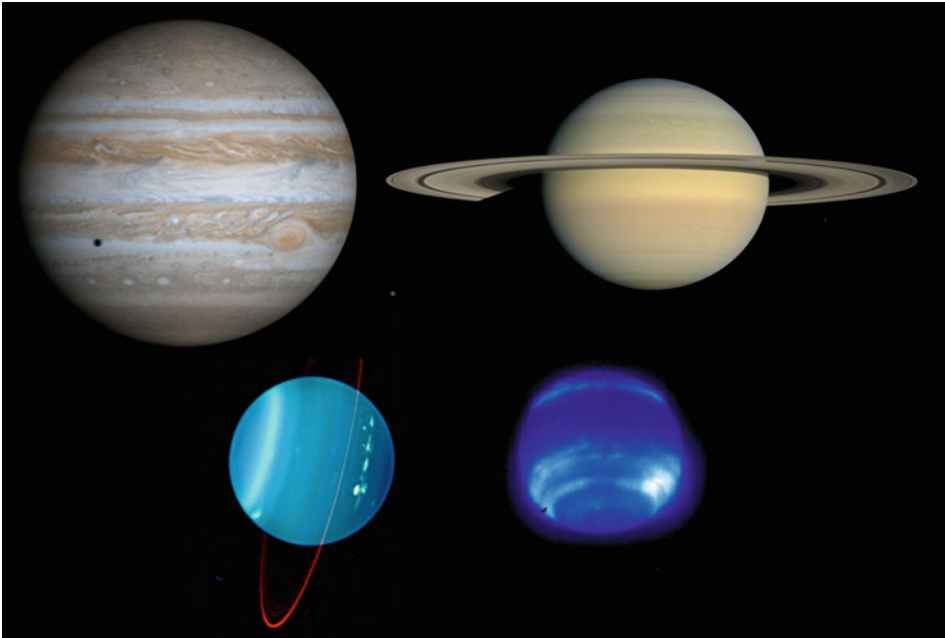
Abstract: The giant planets of the solar system have been studied for centuries using a wide range of remote sensing and in situ techniques. An understanding of the atmospheres of Jupiter, Saturn, Uranus, and Neptune has dramatically improved since the dawn of spacecraft exploration of the outer solar system in the 1970s. Cloud decks that were predicted to exist from thermochemical equilibrium arguments have been observationally confirmed, although the exact vertical distribution of condensible species in these atmospheres remains an active area of study. All four of the giant planets have fast zonal (east-west) winds with prograde and retrograde jets, which dominate their atmospheric circulations. Each planet also contains long-lived cyclonic features or convective cloud features that appear and disappear on short timescales. These features suggest a link between the energy transport in the deep atmosphere and the visible cloud tops; the exact nature of this connection remains an outstanding question in giant planet atmosphere studies. The chemistry of the giant planet atmospheres is driven by both the convective processes that loft disequilibrium species from the deep atmosphere into the stratosphere and the interaction between stratospheric materials and ultraviolet sunlight. A unique opportunity to study these interactions was presented to planetary scientists in 1994, when the 22 fragments of Comet Shoemaker-Levy 9 impacted Jupiter. The future of giant planet atmospheric studies is promising. Several mission concepts that will answer fundamental questions regarding giant planet atmospheres are in various stages of development, and the James Webb Space Telescope will also contribute especially to our understanding of Uranus and Neptune. As an understanding of giant planet formation and evolution expands and deepens, these knowledge gains must be examined against the backdrop of the numerous exoplanet systems recently discovered, very few of which resemble our own.

1 Introduction

The gas giant planets differ in many ways from the rocky planets of the inner solar system. Historically, Jupiter, Saturn, Uranus, and Neptune have been considered to be a class of objects within the solar system unto themselves – they are large, made primarily of gas and ices, they each possess ring systems, and they are orbited by a plethora of moons. More recently, planetary scientists have made the distinction between the larger *gas giants*, Jupiter and Saturn, and the smaller *ice giants*, Uranus and Neptune. [▶ Figure 5-1](#) contains an image montage of the four giant planets of our solar system, and [▶ Table 5-1](#) lists some of the orbital and physical parameters for all four planets.

An examination of [▶ Table 5-1](#) reveals obvious distinctions between the gas giants and ice giants in terms of size, mass, and composition. The masses of Uranus and Neptune are similar to each other, whereas Jupiter and Saturn have widely different masses that are both much larger than those of Uranus and Neptune. Given that the radii of Jupiter and Saturn are not vastly different, this suggests that Jupiter is much more internally compressed than Saturn. The gas giants, Jupiter and Saturn, are composed mostly of hydrogen and helium, while Uranus and Neptune are primarily composed of ices such as methane and water. All four of the giant planets rotate rapidly, resulting in oblateness values that are much larger than those of the terrestrial planets (e.g., the oblateness of Earth is 0.00034).

Two competing models of solar system formation, the *gravitational instability* and the *core accretion* models, are invoked to explain many of the bulk properties of the solar system as



■ Fig. 5-1

Montage of the four giant planets of our solar system (not shown to scale). *Top left*: Jupiter image taken by the Cassini Imaging Science Subsystem on December 7, 2000 (image courtesy of NASA). *Top right*: image of Saturn taken by the Cassini Imaging Science Subsystem on July 23, 2008 (image courtesy of NASA). *Lower left*: Uranus image acquired with the Keck NIRC2 near-infrared camera on July 11–12, 2004 (courtesy of W. M. Keck Observatory). *Lower right*: image of Neptune acquired with the Keck II adaptive optics system and the KCAM near-infrared imager (Max et al. 2003)

well as the general distinctions between the gas giants and the ice giants. The gravitational instability model posits that the protostellar disk became dense enough to be gravitationally unstable and the giant planets formed directly through gravitational collapse of the circumstellar disk. The core accretion model proposes the growth of ice-rock giant planet cores through the collision of planetesimals, followed by gas accretion from the nearby regions of the protosolar nebula. The core accretion model provides a better explanation for the observed nonsolar (enriched) abundances of heavy elements in the outer solar system, but there are still problems with both models that have been highlighted by the discovery of numerous extrasolar planetary systems that do not resemble our own. Despite these new discoveries, the giant planets of our own solar system remain the best laboratories for studying solar system formation and evolution, and these areas have been driving scientific themes in the history of planetary exploration.

The giant planets of the outer solar system have been explored by spacecraft beginning in 1973 with the Pioneer 10 mission to Jupiter. Since that time, all four giant planets have been visited by the Voyager 2 spacecraft, and both Jupiter and Saturn have been explored by orbiters. 📌 [Table 5-2](#) lists the past, present, and planned missions to the giant planets in our solar system.

■ Table 5-1

Orbital, physical, and atmospheric data for the giant planets of the solar system. All data are from de Pater and Lissauer (2001), unless otherwise noted

Parameter	Jupiter	Saturn	Uranus	Neptune
Orbital semimajor axis (AU)	5.20	9.54	19.19	30.07
Mass (10^{24} kg)	1898.6	568.46	86.832	102.43
Equatorial radius ^a (km)	71,492	60,268	25,559	24,766
Oblateness ^b	0.065	0.098	0.023	0.017
Rotation period ^c (h)	9.924	10.543 ^d	17.24	16.11
Obliquity (deg)	3.12	26.73	97.86	29.56
Effective temperature (K)	124.4 ± 0.3	95.0 ± 0.4	59.1 ± 0.3	59.3 ± 0.8
Geometric albedo	0.52	0.47	0.51	0.41
Energy balance ^e	1.67 ± 0.09	1.78 ± 0.09	1.06 ± 0.08	2.61 ± 0.28
H ₂ volume mixing ratio	0.864 ± 0.006	0.963 ± 0.03	0.85 ± 0.05	0.85 ± 0.05
He volume mixing ratio ^f	0.157 ± 0.030	0.034 ± 0.03	0.18 ± 0.05	0.18 ± 0.05
CH ₄ volume mixing ratio ^f	$(2.10 \pm 0.4) \times 10^{-3}$	$(4.5 \pm 2.2) \times 10^{-3}$	0.024 ± 0.01	0.035 ± 0.010

^aRadius is defined to be from the planet center to the 1-bar pressure level

^bOblateness is a function of the equatorial and polar radii and is defined as $(R_e - R_p)/R_e$

^cThe rotation periods of Jupiter and Saturn are given in the System III system, which is referenced to the radio emissions of those planets

^dUpdated value from Cassini observations (Anderson and Schubert 2007); previous value was 10.656 h

^eEnergy balance is defined as the ratio of the energy radiated to space to the amount of solar energy absorbed

^fFrom Niemann et al. (1998)

■ Table 5-2

Missions to the outer solar system

Spacecraft	Target body	Year
Pioneer 10	Jupiter	1973
Pioneer 11	Jupiter	1974
Pioneer 11	Saturn	1979
Voyager 1	Jupiter	1979
Voyager 2	Jupiter	1979
Voyager 1	Saturn	1980
Voyager 2	Saturn	1981
Voyager 2	Uranus	1986
Voyager 2	Neptune	1989
Ulysses	Jupiter	1992 ^a
Galileo	Jupiter	1995–2003
Cassini	Jupiter	2000
Cassini	Saturn	2004–present
New Horizons	Jupiter	2007
Juno	Jupiter	2016 ^b

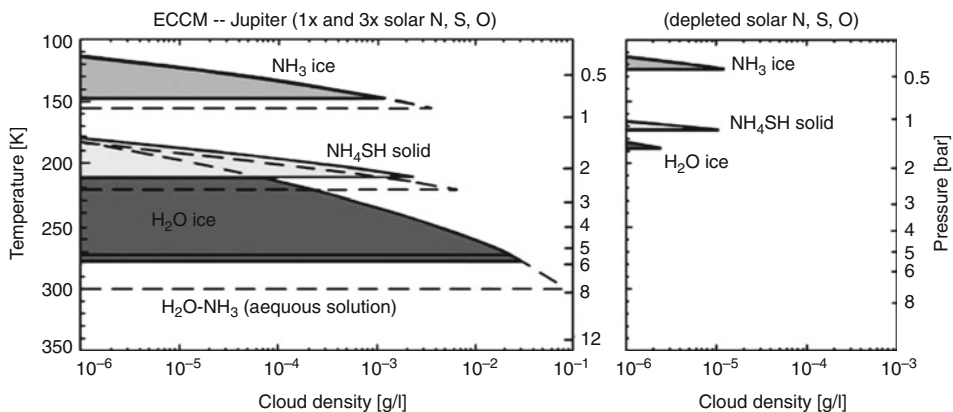
^aHeliophysics mission used to study Jupiter's magnetosphere

^bExpected arrival at Jupiter based on its August 2011 launch

The spacecraft exploration of these large giant worlds of the outer solar system, along with the concomitant ground-based telescopic observations, has yielded numerous answers to outstanding questions about the giant planets and generated at least as many new unanswered questions. However, there are several fundamental areas of study related to giant planet atmospheres in which significantly increased understanding has emerged over the past three decades. The giant planet atmospheric structure, dynamics, and chemistry are key to understanding the physical processes that govern planetary atmospheres in general and will provide important insight into the atmospheres of the newly discovered planets around other stars, which are discussed further in ▶ [Chap. 10](#). ▶ [Section 2](#) of this chapter describes the structure and composition of giant planet atmospheres. In ▶ [Sect. 3](#), the dynamical processes that influence these atmospheres are reviewed, and in ▶ [Sect. 4](#), the role that atmospheric chemistry plays in giant planet atmospheres is discussed. A summary of unanswered questions and future directions in the study of giant planet atmospheres is presented in ▶ [Sect. 5](#). The printed form of this chapter is an abridged version; a more extensive version is available in the online volume of this text.

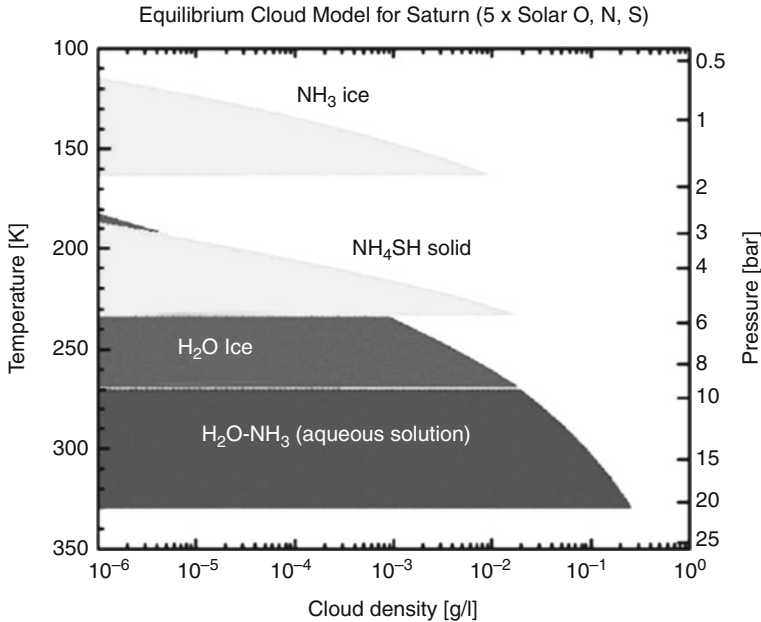
2 Atmospheric Composition and Structure

Clues concerning the composition and vertical structure of the giant planet atmospheres can be found in the protosolar nebula. Based on the chemical abundances of the nebula, out of which the giant planets formed, thermochemical equilibrium models are used to predict the pressure-temperature regimes at which various molecules condense. Using such arguments, Weidenschilling and Lewis (1973) identified the following condensibles on the giant planets: for Jupiter and Saturn, cloud decks of ammonia, ammonium hydrosulfide (NH_4SH), and water are predicted (▶ [Figs. 5-2](#) and ▶ [5-3](#), respectively); for Uranus and Neptune, clouds of methane and



■ Fig. 5-2

Equilibrium cloud condensation model for Jupiter. *Left:* the pressure levels at which Jupiter's three cloud decks form were computed based on the assumption of $1\times$ solar abundances (*solid area*) and $3\times$ solar (*dashed lines*) values. *Right:* Jupiter's cloud deck locations were computed with the following condensible volatiles depleted relative to solar abundances: H_2O , NH_3 , and H_2S (From Atreya and Wong (2005))



■ Fig. 5-3

Equilibrium cloud condensation model for Saturn. The pressure levels at which Saturn's cloud decks form were computed based on the assumption of 5× solar abundances of N, S, and O. Note that in Saturn's atmosphere the condensation of the same species occurs at greater pressure levels than on Jupiter due to the colder temperatures of Saturn's atmosphere. An increasingly larger enrichment in heavy elements as one goes from Jupiter to Neptune is consistent with the core accretion model of planet formation (From Atreya and Wong (2005))

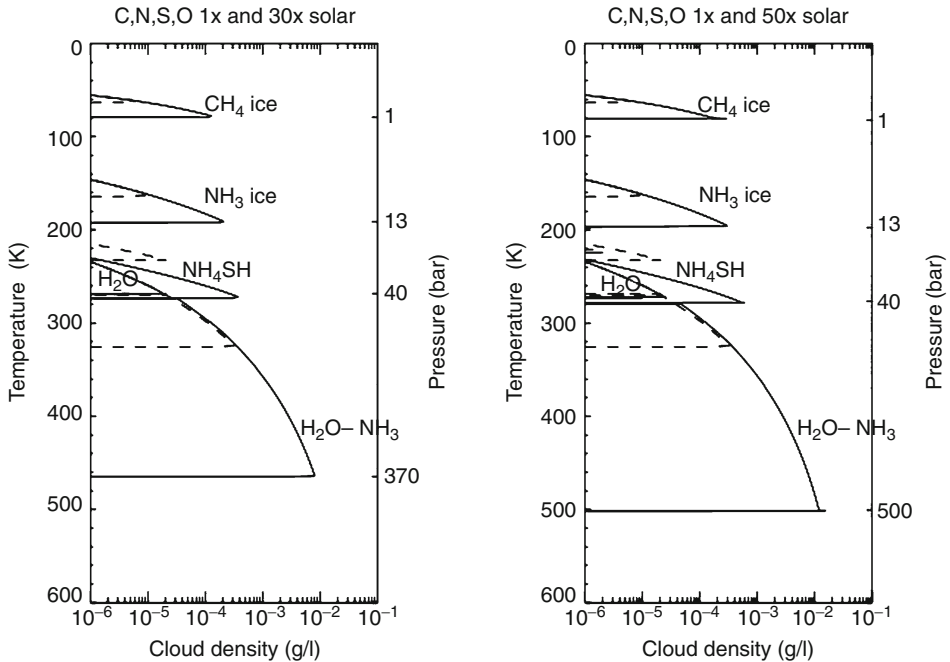
water ice are predicted (► Fig. 5-4). Methane is also present in the atmospheres of Jupiter and Saturn, in smaller abundances than in Uranus and Neptune, but the atmospheric temperatures of the gas giants are warm enough that methane never condenses there.

All of the giant planet atmospheres contain a temperature minimum located at the tropopause; above that, temperatures increase with height due to the absorption of sunlight by stratospheric aerosols and the methane gas absorption bands (► Fig. 5-5). Below the tropopause, temperatures increase with increasing depth as the most efficient means of energy transport is convection and the atmospheric temperature profile is roughly adiabatic. This portion of the atmosphere is heated from below.

In this discussion, we adopt the atmospheric nomenclature defined by West et al. (2004) for the Jovian atmosphere, where a *haze* is defined as a ubiquitous layer of particles smaller than a micron in size and located in the upper troposphere (200–500 mbar) and in the stratosphere ($P < 100$ mbar). We refer to *clouds* when discussing more spatially and temporally variable assemblages of larger particles at deeper levels.

2.1 Cloud Locations

For several decades, the true chemical identities of the clouds in the giant planet atmospheres remained unconfirmed. Although on Jupiter and Saturn the uppermost cloud is assumed to be

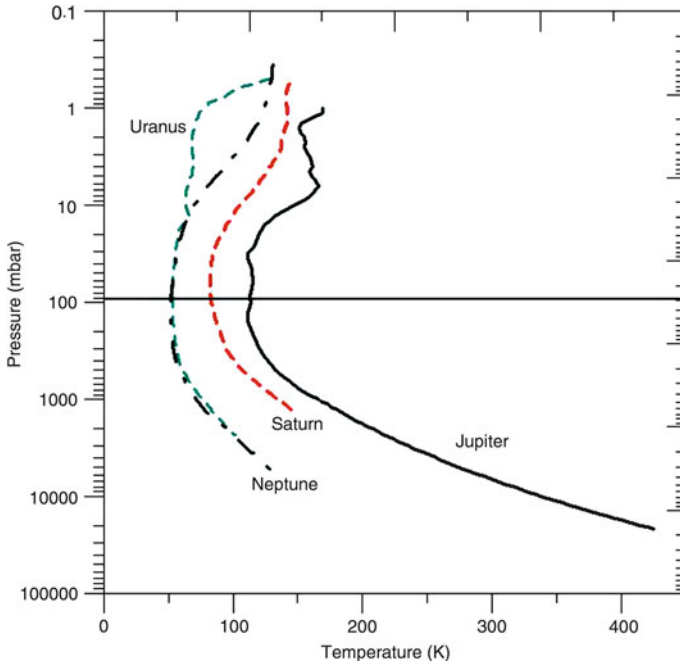


■ Fig. 5-4

Equilibrium cloud condensation model for Neptune, comparing the pressure levels at which Neptune's cloud decks are expected to form when computed assuming $1\times$ (dashed lines) and $30\times$ solar abundances (left panel) and $50\times$ solar values (right panel) for the following condensable volatiles: H_2O , NH_3 , H_2S , and CH_4 . The atmospheric structure for Uranus is likely very similar to that of Neptune since both planets have very similar thermal structures and atmospheric compositions (From Atreya and Wong (2005))

made of ammonia ice based on the thermochemical equilibrium calculations described above, spectroscopic evidence of this remained elusive. It was not until the Galileo mission provided detailed views of the Jovian cloud deck with the Near-Infrared Mapping Spectrometer (NIMS) that spectrally identified ammonia clouds (SIACs) were detected in localized regions on Jupiter (Baines et al. 2002). A $3\text{-}\mu\text{m}$ absorption feature seen in both space-based and ground-based infrared spectra of Jupiter was initially attributed to ammonia (Brooke et al. 1998), but more recent improved model fits suggest a layer of small ammonia-coated particles overlying an optically thicker layer of larger NH_4SH particles (Sromovsky and Fry 2010). The fact that Jupiter's SIACs are short-lived, i.e., last on the order of a few days, seems at odds with the prediction that the upper cloud decks of Jupiter and Saturn are composed of ammonia ice, and suggests that some other process such as photochemical "tanning" or a coating of the pure ammonia ice is commonplace in the giant planet atmospheres.

Confirmation of Jupiter's water cloud also remained challenging. Water vapor was detected on Jupiter using spectroscopic observations from the Voyager and Galileo spacecraft (Carlson et al. 1992; Roos-Serote et al. 1998) as well as airborne telescopes flying high in Earth's atmosphere (Larson et al. 1975; Bjoraker et al. 1986). Since these observations probed to pressure levels ~ 5 bars in the jovian atmosphere, the presence of water vapor was not surprising given



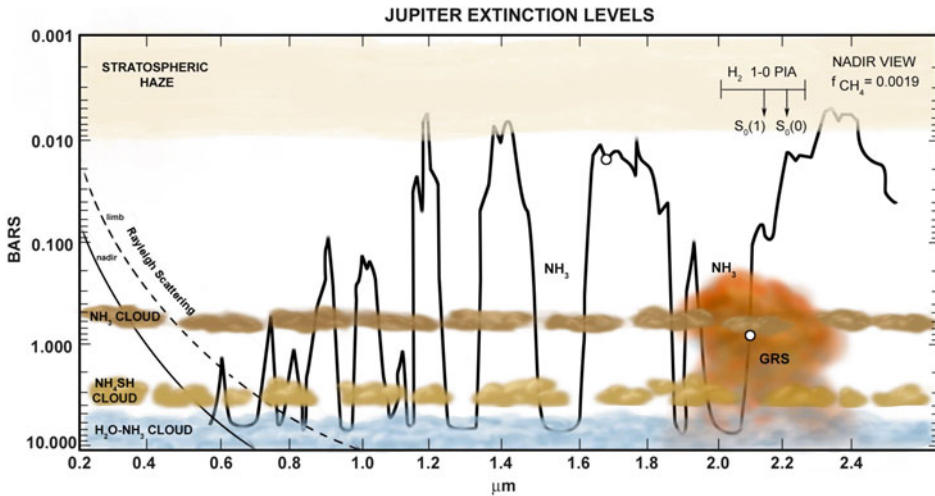
■ Fig. 5-5

Pressure-temperature profiles for all four giant planets. Figure from Sánchez-Lavega (2010); data for each profile were taken from Voyager occultation measurements by Lindal et al. (1981) (Jupiter), Lindal et al. (1985) (Saturn), Lindal et al. (1987) (Uranus), and Lindal et al. (1990) (Neptune). The Jupiter profile also includes data from the Galileo probe measurements by Seiff et al. (1998)

the thermochemistry believed to have taken place in Jupiter's atmosphere. However, it was also expected that Jupiter's vigorous convection should be strong enough to loft water vapor to higher and colder altitudes, where it would condense into ice and be seen above the ammonia cloud deck. Yet no ubiquitous water ice signatures were detected by the Voyager Infrared Interferometer Spectrometer and Radiometer (IRIS) instrument (Hanel et al. 1979).

The presence of water ice on Jupiter was not confirmed until vertical structure studies using Galileo Orbiter imaging data (Banfield et al. 1998; Gierasch et al. 2000) motivated a reexamination of Voyager data. The identification of convective thunderstorm clouds in Galileo and Voyager imagery prompted Simon-Miller et al. (2000) to reexamine the Voyager IRIS data. They found that approximately 1% of the spectra analyzed contained a far-infrared absorption feature attributable to water ice but that the optical depth of the water ice was not large enough to distinguish this cloud against the denser overlying ammonia cloud deck.

The vertical locations, thicknesses, and compositions of the cloud layers in the giant planet atmospheres are determined through vertical structure modeling, which has generally been conducted using two different approaches. Forward modeling techniques assume a basic cloud structure with some number of free parameters that describe the aerosol physical properties, layer thicknesses, and locations. These models use a radiative transfer code to generate synthetic spectra or center-to-limb (CTL) brightness variation curves. These spectra or CTL curves are



■ Fig. 5-6

Extinction levels in Jupiter's atmosphere as a function of wavelength from UV to near IR. Ammonia and H_2 pressure-induced absorption (PIA) features are indicated (From Baines (personal communication))

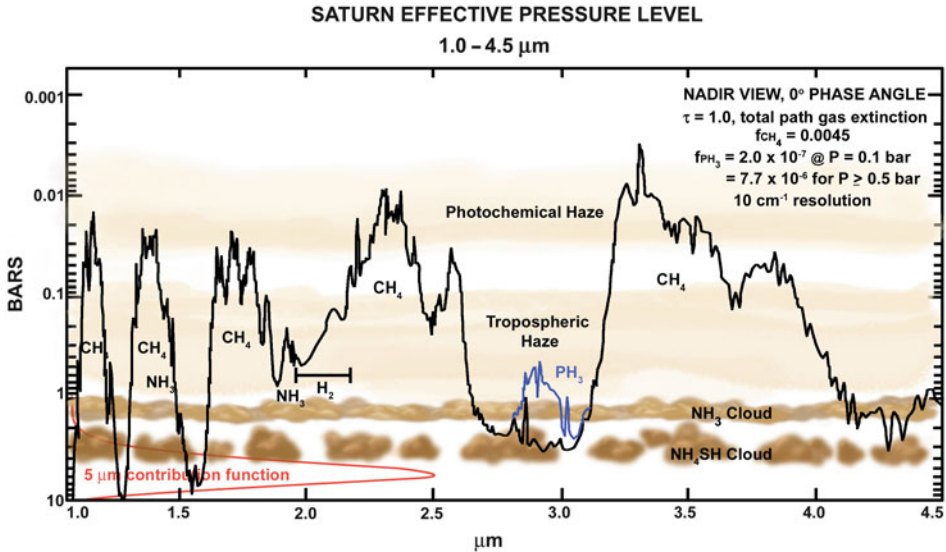
then compared with observations, and the free parameters in the model are subsequently varied iteratively until the synthetic curves or spectra that best match observational data are achieved. An alternative approach is an inversion technique, where inferences about an atmosphere's structure can be made from observational data.

Aerosol optical and radiative properties are determined from remote sensing measurements. Multiwavelength atmospheric radiance measurements are used as inputs to radiative transfer modeling codes, and the physical properties of the aerosol layers (e.g., particle size, optical depth) can be computed. ▶ [Figures 5-6](#) and ▶ [5-7](#) show the depths to which one can sound in the atmospheres of Jupiter and Saturn, respectively, as a function of wavelength.

2.1.1 Limitations of Remote Sensing

The atmosphere of Jupiter is the best-studied among the four giant planets. Jupiter's large size and relative proximity to Earth have enabled amateur and professional astronomers alike to conduct long-term monitoring of the Jovian atmosphere with first photographic and now CCD imaging techniques. A historical record of Jupiter observations can yield important insight into long-term changes in the giant planet atmospheres (Beebe et al. 1989), but such observations are limited in scope. As technologies such as adaptive optics and infrared imaging have improved, so has the demand for observing facilities with such capabilities. Thus, regular access to these new advances over decadal-long time scales has remained a challenge for ground-based giant planet observers.

Historically amateur astronomers have made significant contributions to the study of giant planet atmospheres, earlier through their careful drawings and now more commonly with their photography and digital imagery of Jupiter and Saturn. With modest-sized telescopes



■ Fig. 5-7

Extinction levels in Saturn's atmosphere as a function of near-infrared wavelength. Ammonia, methane, phosphine, and H_2 pressure-induced absorption features are indicated (From Baines (personal communication))

(~25–35 cm mirror diameter) and rapid imaging cameras, amateur observers can produce very high-quality images by taking observations at a very high-time cadence. A small subset of these images is taken in very brief moments of excellent seeing. (This is sometimes referred to as the “lucky imaging” technique, cf. Law et al. 2006.) Postprocessing software is then used to identify the best images out of the gigabytes of data acquired in one night. The amateur observers regularly contribute their images to the Atmospheres Node of the International Outer Planets Watch through its online database, the Planetary Virtual Observatory and Laboratory (PVOL), where the data can be viewed by professional and amateur astronomers worldwide (Hueso et al. 2010). In addition to the long-term monitoring of atmospheric phenomena enabled by this rich historical record, amateur astronomers have been the first to report many significant phenomena in giant planet atmospheres, such as color changes (e.g., the reddening of White Oval BA) and bolide impacts. The PVOL images generally lack absolute photometric calibration and spectral information other than that afforded by broadband and sometimes a methane absorption filter, so their strength primarily lies in their extensive temporal coverage, which can elucidate dynamical changes in the atmospheres of Jupiter and Saturn.

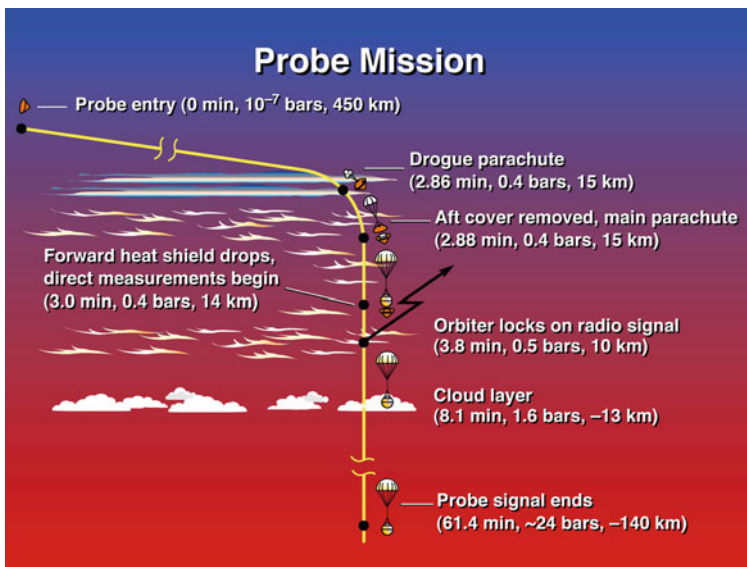
The geometry of the solar system also limits the information one can glean from Earth concerning the physical characteristics (size, shape, scattering properties) of the giant planet aerosols. Large variations in phase angle, or the observer-target-Sun angle, are necessary to accurately quantify the scattering properties of the giant planet aerosols, yet from Earth we are limited to maximum phase angles of $\sim 11^\circ$, 6° , 3° , and 2° for Jupiter, Saturn, Uranus, and Neptune, respectively. Only spacecraft observations can achieve much larger phase angles, and as can be seen from Table 5-2, those opportunities have been limited in number.

Finally, remote sensing observations of the giant planet atmospheres can probe a variety of pressure levels and aerosol layers by capitalizing on the vertical discrimination afforded

by various molecular absorption bands. It remains difficult to accurately sound below the visible cloud deck, though, due to the increasing opacity with depth. Models used to determine atmospheric structure based on cloud reflectivity measurements are often plagued with nonuniqueness problems because variations in several different parameters can produce the same observed effect. For example, to explain the contrasts seen in Jupiter's clouds at continuum wavelengths, two different modeling approaches have been used. Forward modeling studies such as those by West et al. (1986) and Chanover et al. (1997) find that the continuum contrasts are mostly due to spatial variations in the single-scattering albedo of the upper cloud, whereas models used by Banfield et al. (1998) and Sromovsky and Fry (2002) suggest that optical depth variations are largely the cause of cloud contrasts (West et al. 2004). More spacecraft observations over a wide range of wavelengths and phase angles are needed to break this degeneracy.

2.2 In Situ Measurements

The atmosphere of Jupiter is currently the only one of the four giant planets that has been explored via in situ measurements made from an entry probe. The Galileo probe entered Jupiter's atmosphere on December 7, 1995 and descended through the Jovian atmosphere, transmitting data for 61 min before contact was lost when the probe was near the 24-bar pressure level (Young et al. 1996) (► Fig. 5-8). The probe was equipped with an instrument suite designed to characterize Jupiter's inner magnetosphere as well as the atmospheric cloud structure, chemical environment, and wind field. The lightning and radio emission detector (LRD) and the energetic particle instrument (EPI) were used to characterize the energetic particles in the innermost regions of Jupiter's radiation environment. The EPI data were acquired



■ Fig. 5-8

Timeline of events associated with the Galileo probe entry and descent through Jupiter's atmosphere (Image courtesy of NASA)

during the preentry phase of the mission, whereas the LRD operated throughout the descent phase as well. The chemical composition of Jupiter's atmosphere was directly measured with two instruments. The helium abundance detector determined Jupiter's relative helium abundance with greater accuracy than previous estimates, which has important implications for giant planet and solar system formation theories. The neutral mass spectrometer measured mixing ratios of both major and minor species in the Jovian atmosphere as well as isotopic ratios. These in situ measurements were critical for determining the relative contributions of the protosolar nebula and icy planetesimals of the outer solar system to the giant planet atmospheres (Young 2003).

The vertical structure and optical properties of Jupiter's atmosphere were quantified using three instruments: the nephelometer, which was designed to measure the aerosol scattering properties and locations; the atmospheric structure instrument (ASI), which measured the atmospheric thermal structure and vertical winds; and the net flux radiometer (NFR), which was used to determine the vertical distribution of atmospheric heating and cooling and atmospheric opacity throughout the probe's descent phase. Finally, the Galileo probe mission included a Doppler wind experiment (DWE), which was not a separate instrument on board the probe. Rather, the Doppler delay of the probe relay carrier frequency was used to determine the deep zonal winds, i.e., below the cloud decks, in Jupiter's atmosphere.

The Galileo probe entered Jupiter's atmosphere at a latitude of 6.5° N in the North Equatorial Belt, a region characterized by bright white convective plumes and darker, relatively cloud-free, areas of subsidence between the plumes. It descended through Jupiter's atmosphere in one of the interplume downwelling regions (Orton et al. 1998), thus providing an unexpected and likely somewhat atypical picture of the Jovian atmosphere. The Galileo probe measured a helium abundance lower than that expected from the protosolar nebular predictions, which indicates that helium may have gravitationally settled deeper in Jupiter's interior (von Zahn et al. 1998). Neon was found to be severely depleted, while C, N, S, Ar, Kr, and Xe were all measured with $\sim 3\times$ solar abundance. Condensible species such as H_2O , NH_3 , and H_2S were all depleted, which is likely due to the unique nature of the probe entry site (Niemann et al. 1998). The jovian cloud structure sensed by the Galileo probe contained a tenuous cloud with a base at 0.5 bar, a thin but well-defined cloud with a base at 1.4 bar, and another tenuous aerosol layer between ~ 2.4 and 3.6 bars (Ragent et al. 1998; Sromovsky et al. 1998). The lack of detection of a deep water cloud suggests that a dynamical process, i.e., a strong downdraft, was responsible for clearing this region of Jupiter's atmosphere. Jupiter's zonal (east-west) winds appeared to extend down at least to the depth where the probe data collection ceased (Atkinson et al. 1998), but this again may be due to the localized conditions in this downwelling region rather than a result that is broadly applicable to the entire planet. The Galileo probe results were key for improving the understanding of giant planet formation and evolution, and they highlighted the need for in situ measurements of giant planet atmospheres that are complementary to the richer orbiter and ground-based data sets.

3 Atmospheric Dynamics

The dynamics of the giant planet atmospheres are driven by a combination of solar input (which for Saturn, Uranus, and Neptune varies seasonally) and internal heat. Below the cloud decks, the atmospheres of the giant planets are believed to be adiabatic. One of the fundamental questions of giant planet atmospheric dynamics is the manner in which their atmospheric circulations are linked to the abyssal circulations.

3.1 Winds

The winds on the giant planets are the fastest in the solar system. **Figure 5-9** shows the mean zonal (east-west) wind profiles for each of the four Jovian planets. The profiles are all characterized by east-west jets, with prograde equatorial jets for Jupiter and Saturn, which also have a greater total number of jets, and retrograde equatorial jets for Uranus and Neptune. All four of the giant planets exhibit remarkable north-south symmetry in their zonal wind profiles. **Figure 5-10** shows Jupiter's zonal wind profile overlaid on a cylindrical map made from HST images. We see a strong correlation between the zonal wind jet maxima and minima and the banding of Jupiter's clouds, indicating that these jets are responsible for Jupiter's visible appearance.

The meridional (north-south) winds on the giant planets are several orders of magnitude weaker than the zonal winds, indicating that the giant planets' circulation is dominated by east-west motions. As shown in **Table 5-1**, there is considerable variation among the gas giants in terms of both solar insolation and internal heat. This suggests that the forcing of the atmospheric circulation in these planetary atmospheres is largely a function of their formation and rapid rotation.

Uranus is unique among the giant planets in that its equilibrium temperature is quite close to its true disk-averaged temperature (**Table 5-1**). This implies that any internal heat, if it exists, is inefficiently transferred to the observable weather layer. In contrast with Voyager 2

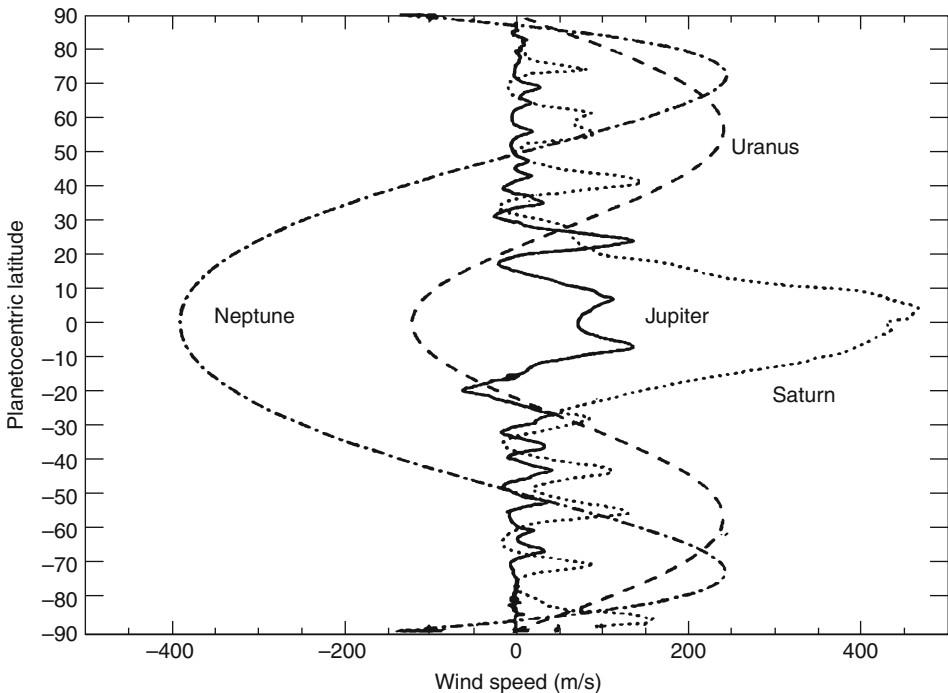
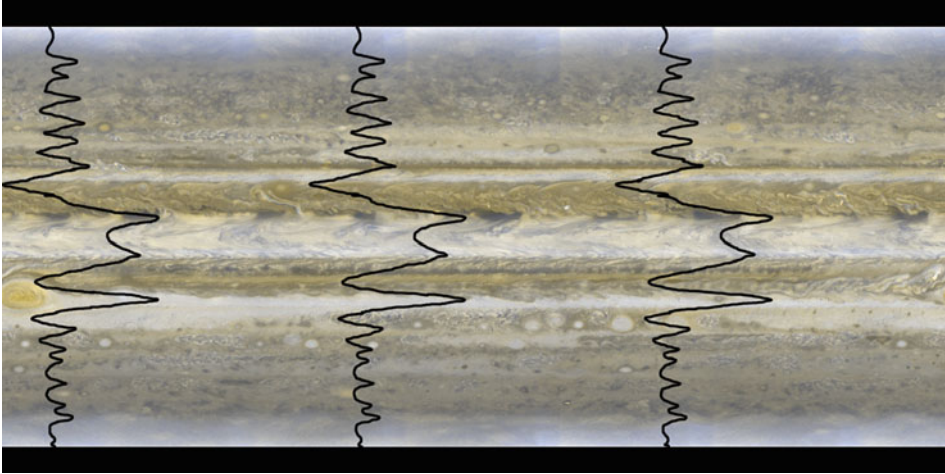


Fig. 5-9

Zonal wind profiles for all four giant planets (Image from Irwin (2009), Fig. 5.2)



■ Fig. 5-10

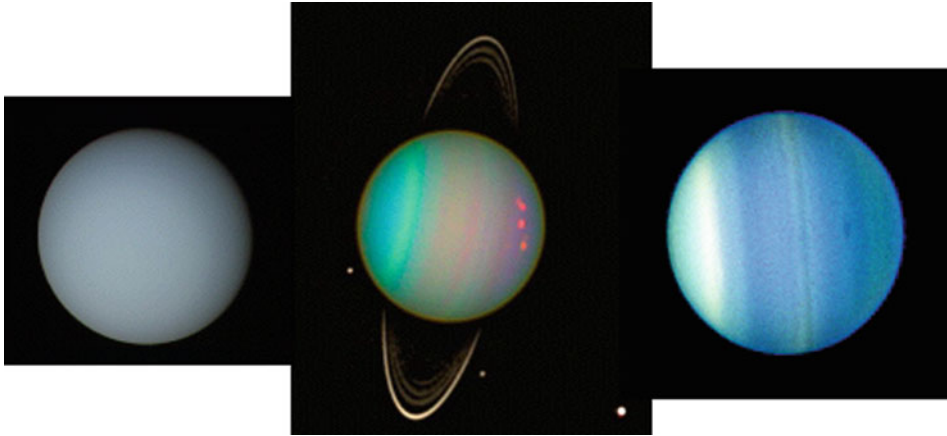
Jupiter's zonal wind profile overlaid on a cylindrical map made from HST images of Jupiter acquired in October 1996 (From Simon-Miller (personal communication))

measurements, which show an adiabatic lapse rate below approximately the 0.1 bar level, deep interior models of Uranus suggest strong molecular gradients that should inhibit convection (Guillot 1999). Thus, even if internal heat within Uranus is substantial, the planet is prevented from following the usual path of heat transfer from its interior used by other gas giants.

It is expected that solar insolation plays a considerable role in the energy budget of Uranus' weather layer. Uranus' ratio of total emitted infrared irradiance to that of absorbed solar heating, as shown in Table 5-1, is significantly less than that found on the other giant planets. Combined with Uranus' extreme axial tilt, seasonal variations of atmospheric dynamics are expected to be significant in the radiative boundary layer and potentially deeper. The current epoch represents a unique opportunity for us to analyze seasonal forcing of atmospheric dynamics, as Uranus reached its equinox in December 2007. Uranus' last equinox took place in 1965, before the advent of modern detectors, thus we are currently in a "new" age for Uranus atmospheric studies, since both its northern and southern hemispheres are receiving roughly equal amounts of sunlight for the first time in 42 years. Neptune, on the other hand, has the largest internal heat contribution to its outgoing flux of all the giant planets. Thus, a comparative study of the role that insolation plays in driving the atmospheric dynamics on the planets with the two extrema in energy balance can reveal important clues to their divergent evolution.

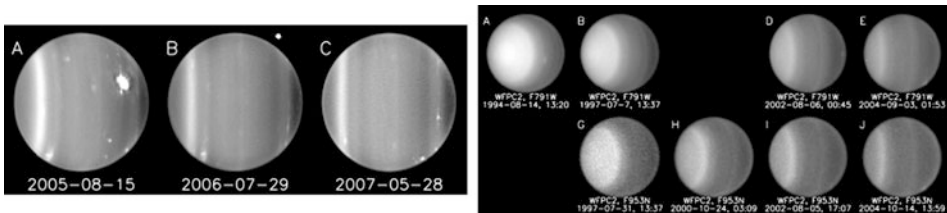
3.1.1 Observational Evidence for Seasonal Changes on Uranus and Neptune

At first glance, a comparison between recent images of Uranus taken near equinox and Voyager 2 images of the planet taken near solstice immediately reveals obvious changes in Uranus' atmosphere (Fig. 5-11). Recent near-infrared imaging with the Keck AO system and the Hubble Space Telescope (Sromovsky and Fry 2005; Hammel et al. 2005) shows an increase in the number of discrete cloud features when compared with 1986 Voyager 2 visible imaging, particularly in the late winter northern hemisphere. However, this comparison is likely



■ Fig. 5-11

Left: image of Uranus taken by the Voyager 2 spacecraft in 1986. *Middle:* image of Uranus taken with ACS on Hubble Space Telescope in 2003. *Right:* image of Uranus taken with ACS on Hubble Space Telescope in 2006 (Images courtesy of NASA)



■ Fig. 5-12

Left: near-IR Keck images of Uranus showing a new bright band forming in Uranus' northern hemisphere, which is seen on the right side of each image. *Right:* HST images illustrating the evolution of Uranus' south polar cap from 1994 to 2004 (All images courtesy of Sromovsky (personal communication))

oversimplified: some of this increase is certainly due to the higher contrast of clouds in the NIR as well as improved visibility of the equatorial latitudes and northern hemisphere as Uranus approaches equinox (Karkoschka 2001). Nonetheless, seasonal change may also play a role in the increase of observable cloud features.

A more compelling argument that seasonal change is occurring on Uranus is the observed asymmetry in the cloud bands, as seen in the right panel of ● Fig. 5-11 as well as in ● Fig. 5-12. The bright band in the southern hemisphere is probably not a permanent feature of Uranus' atmosphere; any fixed pattern would most likely be symmetric about the equator to match the symmetry of the annual average distribution of solar heating within the atmosphere. In fact, a north-south asymmetry is just what would be expected for a seasonal response to solar forcing when that response has a time constant that is long enough to cause a large delay in response but not so long that the response is completely washed out. If the cloud pattern

on Uranus does indeed manifest seasonal change, it should have begun to reverse just before equinox. In fact, that reversal is being seen: the southern band is declining in brightness and a new band is forming in the northern hemisphere (Rages et al. 2007; [Fig. 5-12](#), left panel). The bright polar cap that used to be an obvious feature of the southern hemisphere began to decline even earlier (Rages et al. 2004; [Fig. 5-12](#), right panel), which may indicate a seasonal response with an even shorter time constant.

In addition to the more frequent appearance of discrete clouds and changes in large-scale banded cloud patterns, Uranus' zonal winds may also demonstrate seasonal change. While the Sromovsky and Fry (2005) observations, acquired in 2003 and 2004, show no clear evidence of seasonal change in the zonal winds, Hammel et al. (2005) do find significant changes in wind speeds from 2000 to 2003, with an increase of approximately 30 m/s in the 20–50°N latitude range. This issue requires further study with new observations spanning a wider seasonal coverage, but the possible linkage between zonal winds and seasonally varying insolation is tantalizing.

Radio observations of Uranus at 2 and 6 cm were also suggested to show evidence of seasonal change (Hofstadter and Butler 2003). These wavelengths probe much deeper than visible imaging, down to approximately 50 bars. A pole-to-equator radio brightness gradient has been known to exist even prior to the Voyager 2 flyby. However, while this gradient remained relatively constant from 1981 to 1989, it may have undergone an increase in magnitude between 1989 and 1994. Such a gradient is generally interpreted as an equatorial enhancement in condensable gases such as NH_4SH rather than a true temperature gradient (de Pater et al. 1991). This may imply a Hadley-like circulation in which upwelling gases near the equator condense out while depleted gases are subsiding near the pole ([Fig. 5-13](#)). Thus, an increase in the magnitude of this brightness gradient may indicate a seasonal invigoration of this circulation.

Observations of Uranus between 1 mm and 20 cm do not reveal any *hemispheric* asymmetries, only pole-to-equator variations (Hofstadter, personal communication), suggesting that the processes governing ice giant radio brightnesses differ from those causing the observed variations in reflected sunlight. Neptune, on the other hand, does exhibit hemispheric asymmetries

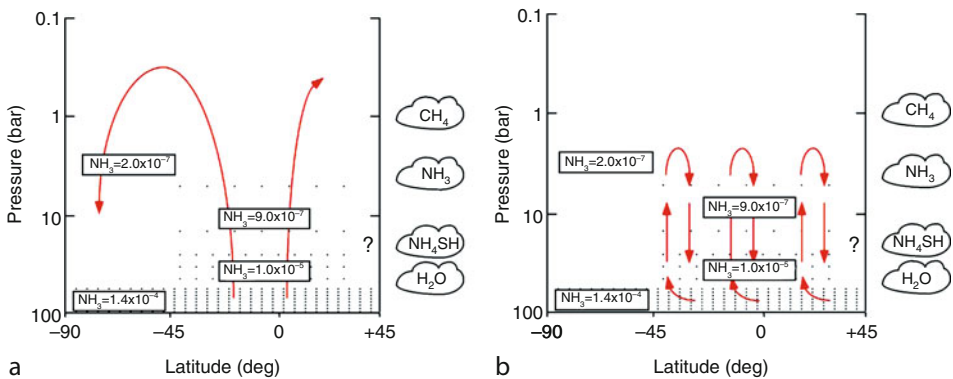


Fig. 5-13

(a) The distribution of absorbers in Uranus' atmosphere required to fit 1994 radio observations. The suggested Hadley-type circulation cell can explain the observed latitudinal gradient. (b) An alternative proposed circulation pattern (Figure from Hofstadter and Butler (2003))

at radio wavelengths. In the early 1990s both of Neptune's polar regions were brighter than its equator. Today, close to southern summer solstice, Neptune's south pole is still radio bright, but the north pole is not visible (Hofstadter, personal communication). The link between seasonal insolation and ice giant atmospheric dynamics clearly warrants further study.

Uranus' extreme axial tilt results in an unusual hemispheric asymmetry in solar energy deposition. Neptune, on the other hand, is an ice giant planet with a more moderate axial tilt of nearly 30° . Although its energy balance is more than twice that of Uranus (► [Table 5-1](#)), Neptune also exhibits long-term atmospheric variations, as evidenced by an increase in disk-averaged brightness (Lockwood and Thompson 2002; Sromovsky et al. 2003). A lagged seasonal model was invoked by Sromovsky et al. (2003) to explain Neptune's long-term brightness changes, which they suggested were caused by Neptune's changing subsolar latitude. However, the long-term photometric record suggests that something other than seasonal change is at work; previous investigators also have considered Neptune's response to the 11-year solar cycle or its changing heliocentric distance (Lockwood and Jerzykiewicz 2006; Hammel and Lockwood 2007) as causes for Neptune's observed temporal variations. It is clear that with a much larger internal heat source than Uranus, along with a weaker solar flux at its greater orbital distance, the role of solar insolation in driving atmospheric dynamics on Neptune may be different than for Uranus.

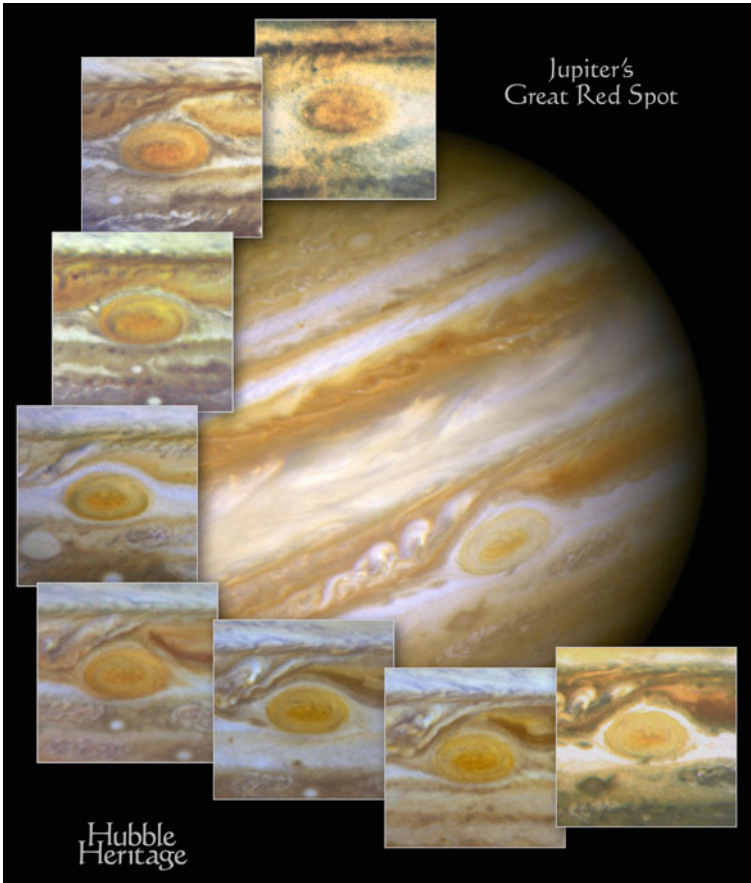
3.2 Storm Features

Convective activity in the giant planet atmospheres is manifested through the apparition of storm features over a wide range of size scales. These features vary in diameter, latitudinal and longitudinal extent, and longevity on each of the giant planets due to the unique aspects of each atmosphere.

3.2.1 Jupiter

The Jovian atmosphere is teeming with cyclonic and anticyclonic storm features. Several of the largest of these features are visible even with low-power ground-based telescopes. The most famous of these storms is the Great Red Spot (GRS), which is more than twice the size of Earth and has been in existence at least since it was first observed more than 150 years ago (► [Fig. 5-14](#)). It is a high-pressure, anticyclonic, counterclockwise-rotating storm system that is maintained at a planetocentric latitude of roughly -25° by a strong prograde jet to its south and a strong retrograde jet to its north.

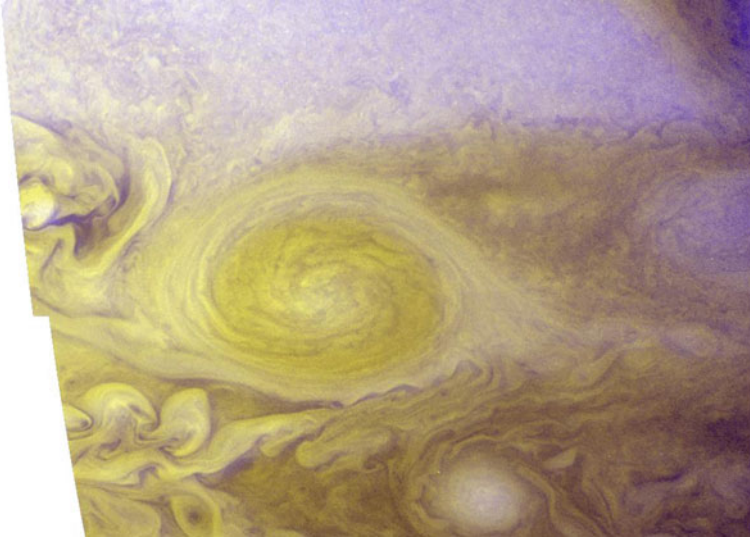
South of the GRS at approximately -30° latitude, three smaller anticyclonic white ovals, named FA, BC, and DE, formed out of the South Temperate Zone (STZ) in 1939. They were first seen following a period when the STZ rapidly clouded over and became a white band; once the clouds subsided, they coalesced into three discrete, rotating storm systems (Peek 1953). In 1998, BC and DE merged to form Oval BE, and in 2000 BE and FA merged to form a single White Oval, BA. The color of BA changed from white to red in 2005 (► [Fig. 5-15](#)). The cause of this color change is not clear, but it may be due to changing dynamics within the oval that resulted in the exposure of reddish condensation nuclei that were lofted from Jupiter's deeper atmosphere Cheng et al. (2008), Perez-Hoyos et al. 2009.



■ Fig. 5-14

Montage of image of Jupiter's Great Red Spot acquired with the Wide Field Planetary Camera 2 on Hubble Space Telescope (Image courtesy of NASA)

The coloration of the GRS and, more recently, Oval BA remains an outstanding mystery in studies of the Jovian atmosphere. West et al. (1986) summarized the state of knowledge at that time by providing two lists of candidate compounds – both organic and inorganic – that could be responsible for the coloration of Jupiter's clouds. These included hydrogen sulfides, allotropes of phosphorus and sulfur, and irradiated mixtures of hydrogen, methane, and ammonia ices. There has been relatively little laboratory work done at conditions appropriate for Jovian pressures and temperatures to confirm or rule out these candidate materials as coloring agents in Jupiter's atmosphere. Two competing hypotheses have been invoked to explain the sources of the coloring agents in the giant planet atmospheres: compounds containing sulfur, phosphorus, hydrogen, and nitrogen that have been convectively transported upward (West et al. 1986) and the coating of ammonia ice particles by photochemically produced hydrocarbons (Atreya et al. 2005; Kalogerakis et al. 2008). High quality multispectral observations of Jupiter's atmosphere, analyzed with numerical techniques such as Principal Component Analysis, indicate



■ Fig. 5-15

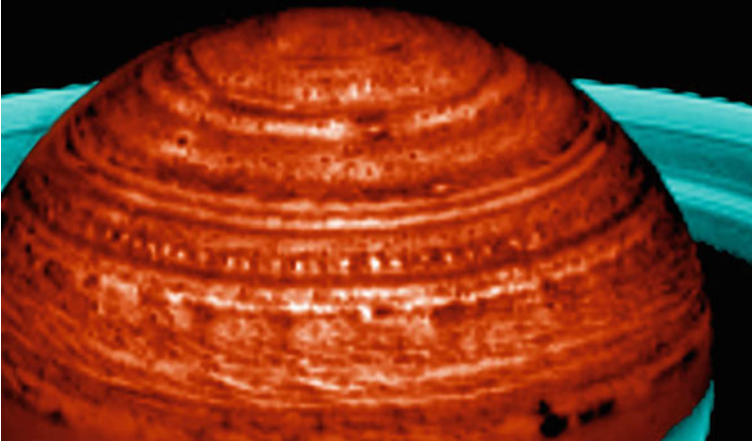
Image of Jupiter's "Little Red Spot," or Oval BA, acquired by the LORRI imager on New Horizons on February 27, 2007 (Image courtesy of NASA)

that several chromophores are needed to explain the spatial variations in the Jovian cloud colors (Simon-Miller et al. 2001a, 2001b; Strycker et al. 2011). However, the exact nature or identity of these chromophores remains unclear. Further analysis that relates particle microphysics, atmospheric dynamics, and local radiation field will shed light on this issue. It is important that we understand the nature of the giant planet chromophores because they are almost surely linked to the dynamics and photochemistry of those atmospheres and may reveal a production mechanism for organic molecules.

3.2.2 Saturn

Imaging Saturn's atmospheric features at high spatial resolution presents a challenge for ground-based telescopes. Until the advent of the CCD cameras in the 1980s, only about a dozen features were clearly detected visually or photographically over a century of observations (Sánchez-Lavega 1982). Typically ground-based CCD imaging in the visual range can detect cloud features on Saturn larger than about 3,000 km if they are located at the sub-Earth point. In addition, they must have sufficient contrast relative to surrounding clouds to be detected. This is difficult on Saturn due to the extinction of reflected sunlight by a dense high-altitude haze layer. The optimal contrast in the optical/CCD wavelength range is found in blue-green and 890 nm methane-band images.

The Voyager 1 and 2 encounters in 1980 and 1981 provided high-resolution images of Saturn's cloud morphology but in a limited spectral range from violet to red wavelengths. Voyager images showed that isolated features are rare in Saturn's atmosphere, but other interesting atmospheric features were seen in the north such as the "ribbon wave" (Sromovsky et al. 1983) and



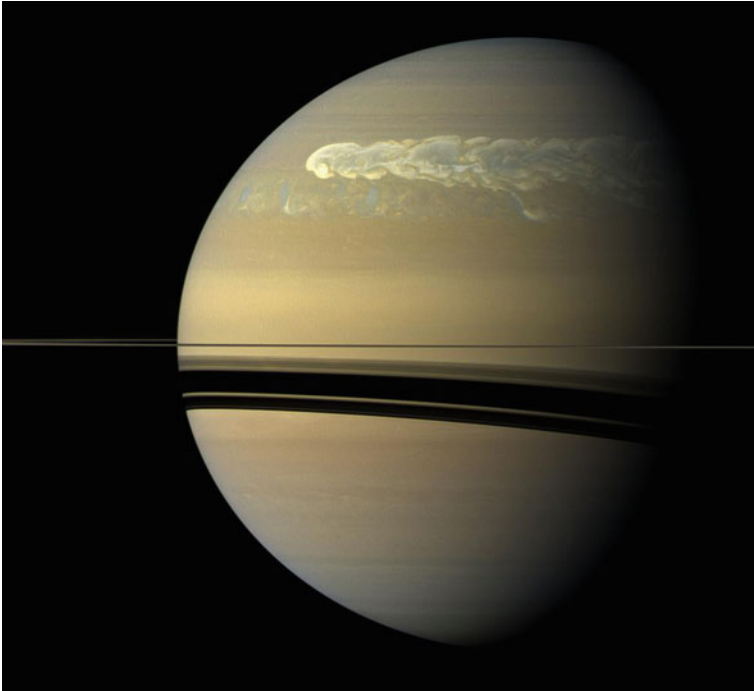
■ Fig. 5-16

Image of Saturn's "string of pearls" cloud formation, taken with Cassini's visual and infrared mapping spectrometer on April 27, 2006 (Image courtesy of NASA)

the "polar hexagon" (Godfrey 1988). Newer Cassini data revealed high quality observations of Saturn's north polar hexagon and vortices at both poles (Baines et al. 2009, Dyudina et al. 2009), as well as additional phenomena such as the "string of pearls" (🔍 Fig. 5-16), which shows regularly spaced clearings in the clouds (the bright regions in the infrared image in 🔍 Fig. 5-16). This appears to be a manifestation of a planetary-scale wave and is likely linked to the deeper circulation in Saturn's atmosphere.

Saturn's atmosphere also undergoes localized convective activity roughly every 30 years, which corresponds to approximately once per Saturnian year. These convective outbursts are manifested by the development of gigantic storm systems known as Great White Spots (Sánchez-Lavega 1982). A major event occurred in the northern equatorial region in 1990 and was studied both from the ground and with Hubble Space Telescope (Sánchez-Lavega et al. 1991; Beebe et al. 1992; Barnet et al. 1992; Westphal et al. 1992). The cloud tops of this storm were convectively lofted to more than a scale height above the surrounding cloud deck, and the resultant increase in cloud optical depth of Saturn's equatorial region persisted for several years after the outbreak.

More recently, a major storm outbreak occurred in the northern midlatitudes. It was first detected through ground-based observations on December 5, 2010, at a planetographic latitude of 38° and, within the span of 1 week, expanded to a linear size of $\sim 8,000$ km (Sánchez-Lavega et al. 2011). This time, the Cassini spacecraft was wellpositioned in its orbit around Saturn to study the storm and its evolution with its imaging and spectroscopic instrument suite. 🔍 Figure 5-17 shows the storm as imaged by Cassini's Imaging Science Subsystem roughly 2.5 months after the storm was first detected. Thermal infrared imaging and spectroscopy revealed that this storm penetrated vertically well into Saturn's stratosphere, which resulted in heating as the material fell back onto Saturn's upper atmosphere (Fletcher et al. 2011). Outbreaks such as these provide a unique opportunity to study the zonal wind structure and vertical energy transport in Saturn's atmosphere.



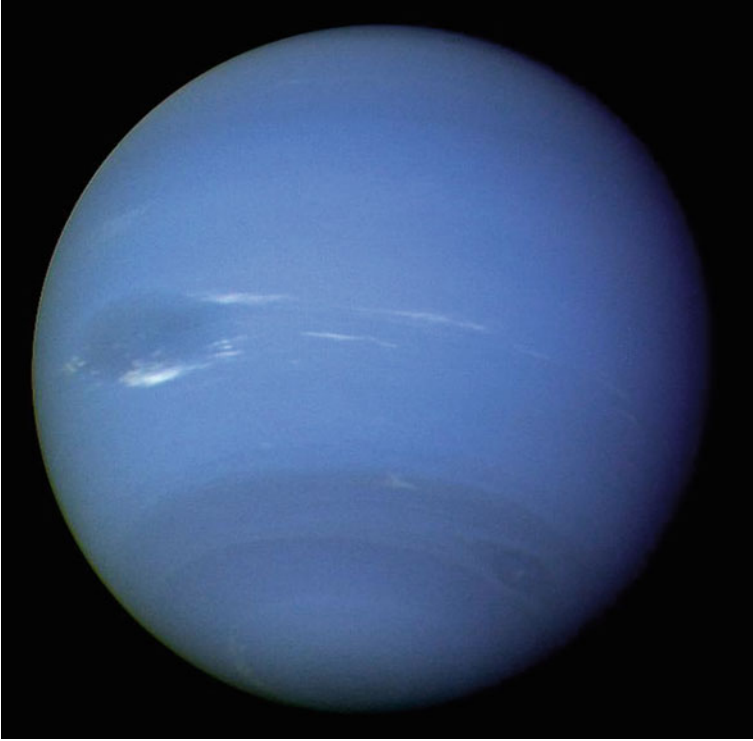
■ Fig. 5-17

Image of the recent storm in Saturn's northern hemisphere, taken with Cassini's Imaging Science Subsystem wide-angle camera on February 25, 2011 (Image courtesy of NASA)

3.2.3 Uranus and Neptune

When Voyager 2 flew by Uranus in 1986 during southern summer solstice, the planet lacked significant storm clouds and atmospheric features. Only through a radical adjustment of image contrast and dynamic range could several faint storm systems be discerned in the Voyager 2 data. However, over the past decade the atmosphere of Uranus has become much more active, now revealing numerous short-lived convective storm features. The cause of these changes is not entirely clear, although seasonal variation in insolation is likely a significant factor. Since Uranus reached equinox in December 2007, over the past decade its northern hemisphere began to receive direct sunlight after a period of several decades in darkness.

The application of new technologies to the study of Uranus' atmosphere also aided in the detection of new small storm features. The Keck telescopes, equipped with adaptive optics system, have enabled diffraction-limited imaging of Uranus in the near-IR, where the contrast between convective storm features and the methane clouds is greatest. The Hubble Space Telescope has also provided high spatial resolution imagery of the Uranian atmosphere from optical through near-IR wavelengths, including the first detection of a dark spot on Uranus in 2006 (Hammel et al. 2009). A large bright complex of clouds was seen to migrate in latitude with an inertial oscillation superimposed on the zonal flow (Sromovsky et al. 2007), and another long-lasting southern feature migrated toward the equator, where it met its eventual demise



■ Fig. 5-18

Image of Neptune taken by the Voyager 2 narrow-angle camera on August 16 and 17, 1989 (Image courtesy of NASA)

(de Pater et al. 2011). These interactions hint at a coupling between giant planet zonal circulation and convective motion, which should be explored further as the planet moves toward its next solstice.

Neptune's atmosphere has demonstrated convective activity regularly since the time of the Voyager 2 encounter in 1989. A large disturbance dubbed the Great Dark Spot was seen in Voyager 2 imagery (► Fig. 5-18), but this disturbance along with its accompanying white clouds did not persist for decades; they were gone by the time HST observed Neptune in 1994 (Hammel et al. 1995). Neptune is also expected to undergo seasonal variations due to its nonzero axial tilt, and continued observations over the next several years will likely reveal new features and changes in zonal wind structure due to its slowly varying insolation.


4 Atmospheric Chemistry

The distribution of chemical species in the atmospheres of the giant planets is governed by several different processes depending on altitude. In the troposphere, where the temperature gradient is negative, convection is the dominant means of energy transport. Species transport

is relatively rapid; molecules that are formed at depth through thermochemical equilibrium reactions and condensation can be lofted to altitudes where their interactions with ultraviolet sunlight can change their properties. An example of this kind of reaction is the proposed “tanning” of ammonia ice particles by solar UV radiation after they have been transported vertically from deeper in the atmosphere (discussed above as a proposed mechanism for the coloration of Jupiter’s reddish clouds).

In the stratosphere, above the temperature minimum, the temperature gradients in the giant planets are positive and/or isothermal, which inhibits vertical motions and results in slow vertical transport of species. In this case, photochemical disequilibrium processes play a significant role in determining the composition of the giant planet stratospheres. For example, gaseous methane in Jupiter’s atmosphere undergoes photochemical reactions to produce hydrocarbons such as ethane (C_2H_6), acetylene (C_2H_2), and ethylene (C_2H_4).

4.1 Energy Balance

The temperatures in the stratospheres of the giant planets can be derived using both indirect and direct techniques. A commonly used indirect method is the observation of occultations. An atmospheric occultation is where the attenuation of a source, such as a background star or a spacecraft radio signal, is observed as the planetary atmosphere passes in front of (or occults) the source. Atmospheric occultations provide measurements of the density structure of an atmosphere through the inversion of the observed light curves. From the density information, a temperature profile can be inferred. This indirect method of obtaining stratospheric temperatures was highly effective for obtaining temperature profiles of all four giant planets during the Voyager missions (shown in  Fig. 5-5). Stellar occultations continue to be employed by orbiters (e.g., Cassini) and ground-based observers as a means of exploring temporal and spatial variations in the atmospheric temperature structure of the giant planets.

Temperatures in the giant planet stratospheres can also be obtained through observations of emission spectra in both the UV and IR spectral regimes. Such observations reveal that the stratospheric temperatures of the giant planets are remarkably uniform with latitude, which suggests that the meridional transport of radiation at these altitudes is very efficient. The energy balance of the giant planet stratospheres is controlled by the heating and cooling by photochemically produced species. For example, on Jupiter, ethane emission is the dominant cooling mechanism between pressures of ~0.2 and 20 mbar.

4.2 Case Study: Shoemaker-Levy 9 Impacts on Jupiter

Photochemical models indicate that methane photochemistry dominates the production of hydrocarbons in the giant planet stratospheres. Yet the detection of some species, such as H_2O and CO , cannot be explained through traditional photochemical pathways, suggesting that the source of these materials must be exogenic. Delivery mechanisms such as comets and interplanetary dust particles have been suggested as a means of supplying the giant planet stratospheres with these molecules (Moses et al. 2000 and references therein).

In 1994, planetary scientists worldwide had a unique opportunity to view such a delivery event in real time. Comet Shoemaker-Levy 9, which had passed close enough to Jupiter in 1992 to be broken up into 22 fragments, impacted Jupiter between July 16 and 22, 1994.

Observations of these impacts were made with all available ground-based and space-based telescopic assets, including HST and Galileo, which resulted in new insight concerning cometary structure and composition, ballistic impact physics, and Jupiter's atmospheric response to these impacts. The temporal evolution of the particulates associated with each impact confirmed the decay of Jupiter's zonal winds with height, while the spectroscopic measurements confirmed that cometary impacts are likely significant contributors to Jupiter's stratospheric CO budget (Lellouch et al. 1997). Although impact events such as this – where astronomers worldwide had more than a year to prepare for their observations – are likely exceedingly rare, the unique physics and chemistry probed by the SL9 impacts highlighted the importance of regular monitoring observations, rapid response capabilities, follow-up observations, and international coordinated efforts where possible.

5 Future Directions

5.1 Unanswered Questions

Fueled in part by the fantastic new discoveries made in the field of giant planet atmospheres over the past several decades, numerous outstanding questions remain. In particular, we hope that over the next few decades, progress will be made in addressing the following issues:

- The water abundance in the atmospheres of the gas giants
- The source of the coloration in the clouds of Jupiter
- The linkage between the giant planets' zonal circulations at the cloud-top level and the deep abyssal circulation
- The role that seasonally varying insolation plays in the vertical structure, cloud chemistry and microphysics, and dynamics of giant planet atmospheres

Advances in understanding these issues can be made through additional observations as we continue to push the instrumental limits of spectral grasp, spectral resolution, spatial resolution, and temporal coverage. Computational modeling of atmospheric dynamics on all scales, ranging from the smallest vortices to the global circulations, will also be critical for advancing the understanding of giant planet atmospheres.

5.2 Future Missions to the Outer Solar System

The Cassini spacecraft reached Saturn in 2004 and continues to provide magnificent views of Saturn's atmosphere. The nominal Cassini mission was scheduled to operate from 2004 to 2008. Due to its extraordinary success, NASA extended it for two more years for the Cassini Equinox mission (2008–2010). It was recently extended again for the Cassini Solstice mission and is currently scheduled to operate in this third phase from 2010 to 2017. The second extension of the Cassini mission will enable planetary astronomers to study the atmosphere of Saturn over half of a year, from northern winter solstice to northern summer solstice, with unprecedented detail. Seasonal changes in Saturn's atmosphere are thought to be caused by the rings, which cast shadows on the atmosphere and shield some of the planet from direct sunlight. The instruments on board Cassini can assess seasonal changes in atmospheric temperatures, composition, and dynamics, and further study new questions about Saturn's atmosphere that arose during the

Cassini Prime mission (e.g., looking for seasonal change in lightning activity rates or in the structure of Saturn's south polar vortex). The final 42 orbits of the 155-orbit Solstice mission will be spent in the proximal orbit phase, where the orbit of the spacecraft will transition to a more elliptical, polar orbit where the spacecraft regularly passes through Saturn's ring plane. This will enable the study of Saturn's internal structure in a fashion analogous to the future Juno mission to Jupiter and will enable a comparative study of the interiors of the two large gas giant planets in our solar system.

The Juno mission to Jupiter was launched in August 2011 and will reach Jupiter in 2016, at which point the spacecraft will enter a highly elliptical polar orbit. Juno will orbit Jupiter 32 times over the 15-month span of the mission; the instrument suite on board the spacecraft is designed to provide new insight into Jupiter's internal structure and global water abundance. The internal mass distribution of the solar system's largest planet will be determined by precisely mapping Jupiter's gravitational field. Obtaining a better estimate for the mass of Jupiter's core will enable planetary scientists to distinguish between the two prevailing theories of giant planet formation: whether Jupiter started with a massive core whose gravity attracted all of the nearby gas or whether the planet formation was triggered by the collapse of an unstable region in the protosolar nebula.

Knowledge of Jupiter's deep water abundance is another key ingredient for solar system and giant planet formation theories, as it has implications for the methods by which volatile compounds were distributed throughout the solar system by icy planetesimals or protoplanets. Juno will measure Jupiter's deep water abundance with a microwave radiometer, which is sensitive to emission coming from Jupiter's atmosphere at depths much greater than those sounded by the Galileo probe.

Jupiter's polar magnetosphere and auroral emissions will be characterized for the first time by Juno, using infrared and ultraviolet remote sensing instruments while simultaneously directly sampling the charged particles and magnetic field near the poles. The entire magnetic field of Jupiter will be mapped over the course of the mission, which will provide an indication of how deep in the planet the magnetic field is generated and will yield new insight into dynamo physics.

The European Space Agency (ESA) recently announced the selection of the Jupiter Icy Moons Explorer, or JUICE mission, for launch early in the next decade. This will be an orbiter whose primary objective will be to study Ganymede, Europa, and Callisto, the large icy satellites of Jupiter. Although the science objectives are focused on satellites, observations of Jupiter's atmosphere would also be possible and would provide new insight into the structure and dynamics of the Jovian atmosphere. Assuming a somewhat standard instrument suite of a wide- and narrow-angle camera, a visible-infrared spectrometer, a thermal infrared and/or ultraviolet spectrometer, and a submillimeter or microwave sounder, this mission may be able to characterize the abundances of minor species (particularly ammonia and water) in Jupiter's troposphere and stratosphere, which has implications for the origin and evolution of giant planet atmospheres. The Jovian atmospheric dynamics and structure also can be characterized through studies of winds, cloud features, atmospheric waves, and tropospheric and stratospheric temperatures.

The James Webb Space Telescope (JWST), which is scheduled to be launched in the next decade, will provide unprecedented infrared observations of Uranus and Neptune. Both Jupiter and Saturn may be too bright to be observed with JWST in its standard imaging and spectroscopic modes, although perhaps through clever techniques such as binning and/or subframing new observations of the gas giant atmospheres will be possible. The spectral coverage afforded by JWST extends that of HST into the infrared, and its 6.5-m diameter

primary mirror will offer a significant increase in spatial resolution over the infrared Spitzer Space Telescope. Through observations of the ethane, methane, and acetylene emissions in the stratospheres of Uranus and Neptune, we will gain an improved understanding of the heating mechanisms in ice giant atmospheres.

Finally, there are several giant planet missions that were recommended as part of the National Academy of Sciences planetary science decadal survey entitled *Vision and Voyages for Planetary Science in the Decade 2013–2022*. This new decadal survey identifies the most important scientific questions in planetary science and provides a prioritized list of flight investigations that can address these fundamental science questions. After the top priority Mars sample return flagship mission, two outer solar system missions were recommended as second and third priorities for flagships in the next decade: a Europa/Jupiter mission and a Uranus system. The decadal survey also recommended five possible missions for the New Frontiers class, including a shallow Saturn probe mission that will yield fundamental new insight into Saturn's atmospheric structure and water abundance.

5.3 Links to Exoplanets

Over the last 15 years, the study of giant planets has been completely revolutionized by the discovery of hundreds of large (Jupiter-sized or larger) extrasolar planets. These planets, many of which orbit their host stars at distances closer than 1 AU, have forced a reexamination of old ideas of giant planet formation and evolution. A deeper understanding of our own solar system and its evolution since the time of formation is critical for understanding these exciting, newly discovered planetary systems elsewhere in the Milky Way galaxy.

Acknowledgments

It is a pleasure to thank R. Beebe, M. Sussman, R. Carlson, P. Strycker, and C. Miller for valuable discussions.

Cross-References

▶ [Exoplanet Detection Methods](#)

References

- | | |
|---|---|
| Atkinson, D. H., Pollack, J. B., & Seiff, A. 1998, <i>J. Geophys. Res.</i> , 103, 22911 | Baines, K. H., Carlson, R. W., & Kamp, L. W. 2002, <i>Icarus</i> , 159, 74 |
| Atreya, S. K., & Wong, A. S. 2005, <i>Space Sci. Rev.</i> , 116, 121 | Baines, K. H., Momary, T. W., Fletcher, L. N., Showman, A. P., Roos-Serote, M., Brown, R. H., Buratti, B. J., Clark, R. N., & Nicholson, P. D. 2009, <i>Planet. Space Sci.</i> 57, 1671 |
| Atreya, S. K., Wong, A. S., Baines, K. H., Wong, M. H., & Owen, T. C. 2005, <i>Planet. Space Sci.</i> , 53, 498 | Banfield, D., Gierasch, P. J., Bell, M., Ustinov, E., Ingersoll, A. P., Vasavada, A. R., West, R. A., & Belton, M. J. S. 1998, <i>Icarus</i> , 135, 230 |
| Anderson, J. D. & Schubert, G. 2007, <i>Science</i> , 317, 1384 | |

- Barnet, C. D., Westphal, J. A., Beebe, R. F., & Huber, L. F. 1992, *Icarus*, 100, 499
- Beebe, R. F., Orton, G. S., & West, R. A. 1989, in *Time-Variable Phenomena in the Jovian System*, ed. M. J. S. Belton et al. (Washington, DC: NASA SP-494), 245
- Beebe, R. F., Barnet, C., Sada, P. V., & Murrell, A. S. 1992, *Icarus*, 95, 163
- Bjoraker, G. L., Larson, H. P., & Kunde, V. G. 1986, *Astrophys. J.*, 311, 1058
- Brooke, T. Y., Knacke, R. F., Encrenaz, T., Drossart, P., Crisp, D., & Feuchtgruber, H. 1998, *Icarus*, 136, 1
- Carlson, B. E., Lacin, A. A., & Rossow, W. B. 1992, *Astrophys. J.*, 388, 648
- Chanover, N. J., Kuehn, D. M., & Beebe, R. F. 1997, *Icarus*, 128, 294
- Cheng, A. F., Simon-Miller, A. A., Weaver, H. A., Baines, K. H., Orton, G. S., Yanamandra-Fisher, P. A., Mousis, O., Pantin, E., Vanzi, L., Fletcher, L. N., Spencer, J. R., Stern, S. A., Clarke, J. T., Mutchler, M. J., & Noll, K. S. 2008, *AJ*, 135, 2446
- de Pater, I., & Lissauer, J. J. 2001, *Planetary Sciences* (Cambridge, UK: Cambridge University Press)
- de Pater, I., Romani, P. N., & Atreya, S. K. 1991, *Icarus*, 91, 220
- de Pater, I., Sromovsky, L. A., Hammel, H. B., Fry, P. M., LeBeau, R. B., Rages, K., Showalter, M., & Matthews, K. 2011, *Icarus*, 215, 332
- Dyudina, U. A., Ingersoll, A. P., Ewald, S. P., Vasavada, A. R., West, R. A., Baines, K. H., Momary, T. W., Del Genio, A. D., Barbara, J. M., Porco, C. C., Achterberg, R. K., Flasar, F. M., Simon-Miller, A. A., & Fletcher, L. N. 2009, *Icarus*, 202, 240
- Fletcher, L. N., Hesman, B. E., Irwin, P. G. J., Baines, K. H., Momary, T. W., Sanchez-Lavega, A., Flasar, F. M., Read, P. L., Orton, G. S., Simon-Miller, A., Hueso, R., Bjoraker, G. L., Mamoutkine, A., del Rio-Gaztelurrutia, T., Gomez, J. M., Buratti, B., Clark, R. N., Nicholson, P. D., & Sotin, C. 2011, *Science*, 332, 1413
- Gierasch, P. J., Ingersoll, A. P., Banfield, D., Ewald, S. P., Helfenstein, P., Simon-Miller, A., Vasavada, A., Breneman, H. H., Senske, D. A., & Galileo Imaging Team 2000, *Nature*, 403, 628
- Godfrey, D. A. 1988, *Icarus*, 76, 335
- Guillot, T. 1999, *Science*, 286, 72
- Hammel, H. B., & Lockwood, G. W. 2007, *Icarus*, 186, 291
- Hammel, H. B., Lockwood, G. W., Mills, J. R., & Barnet, C. D. 1995, *Science*, 268, 5218
- Hammel, H. B., de Pater, I., Gibbard, S. G., Lockwood, G. W., & Rages, K. 2005, *Icarus*, 175, 534
- Hammel, H. B., Sromovsky, L. A., Fry, P. M., Rages, K., Showalter, M., de Pater, I., van Dam, M. A., LeBeau, R. P., & Deng, X. 2009, *Icarus*, 201, 257
- Hanel, R. A., Conrath, B., Flasar, M., Kunde, V., Lowman, P., Maguire, W., Pearl, J., Pirraglia, J., Samuelson, R., Gautier, D., Gierasch, P., Kumar, S., & Ponnamperuma, C. 1979, *Science*, 204, 972
- Hofstadter, M. D., & Butler, B. J. 2003, *Icarus*, 165, 168
- Hueso, R., Legarreta, J., Pérez-Hoyos, S., Rojas, J. F., Sánchez-Lavega, A., & Morgado, A. 2010, *Planet. Space Sci.*, 58, 1152
- Irwin, P. G. J. 2009, *Giant Planets of Our Solar System: Atmospheres, Composition, and Structure* (2nd ed.; Chichester, UK: Praxis)
- Kalogerakis, K. S., Marschall, J., Oza, A. U., Engel, P. A., Meharchand, R. T., & Wong, M. H. 2008, *Icarus*, 196, 202
- Karkoschka, E. 2001, *Icarus*, 151, 84
- Larson, H. P., Fink, U., Treffers, R., & Gautier, T. N., III 1975, *Astrophys. J.*, 197, L137
- Law, N. M., Mackay, C. D., & Baldwin, J. E. 2006, *Astron. Astrophys.*, 446, 739
- Lellouch, E., Bézard, B., Moreno, R., Bocklélé-Morvan, D., Colom, P., Crovisier, J., Festou, M., Gautier, D., Marten, A., & Paubert, G. 1997, *Planet. Space Sci.*, 45, 1203
- Lindal, G. F., Wood, G. E., Levy, G. S., Anderson, J. D., Sweetnam, D. N., Hotz, H. B., Buckles, B. J., Holmes, D. P., Doms, P. E., Eshleman, V. R., Tyler, G. L., & Croft, T. A. 1981, *J. Geophys. Res.*, 86, 8721
- Lindal, G. F., Sweetnam, D. N., & Eshleman, V. R. 1985, *Astron. J.*, 90, 1136
- Lindal, G. F., Lyons, J. R., Sweetnam, D. N., Eshleman, V. R., & Hinson, D. P. 1987, *J. Geophys. Res.*, 92, 14987
- Lindal, G. F., Lyons, J. R., Sweetnam, D. N., Eshleman, V. R., & Hinson, D. P. 1990, *Geophys. Res. Lett.*, 17, 1733
- Lockwood, G. W., & Jerzykiewicz, M. 2006, *Icarus*, 180, 442
- Lockwood, G. W., & Thompson, D. T. 2002, *Icarus*, 156, 37
- Max, C. E., Macintosh, B. A., Gibbard, S. G., Gavel, D. T., Roe, H. G., de Pater, I., Ghez, A. M., Acton, D. S., Lai, O., Stomski, P., & Wizinowich, P. L. 2003, *Astron. J.*, 125, 364
- Moses, J. I., Lellouch, E., Bézard, B., Gladstone, G. R., Feuchtgruber, H., & Allen, M. 2000, *Icarus*, 145, 166
- Niemann, H. B., Atreya, S. K., Carignan, G. R., Donahue, T. M., Haberman, A., Harpold, D. N., Hartle, R. E., Hunten, D. M., Kasprzak, W. T., Mahaffy, P. R., Owen, T. C., & Way, S. H. 1998, *J. Geophys. Res.*, 103(E10), 22831
- Orton, G. S., Fisher, B. M., Baines, K. H., Stewart, S. T., Friedson, A. J., Ortiz, J. L., Marinova, M., Ressler, M., Dayal, A., Hoffmann, W., Hora, J.,

- Hinkley, S., Krishnan, V., Masanovic, M., Tesic, J., Tziolas, A., & Parija, K. C. 1998, *J. Geophys. Res.*, 103, 22791
- Peek, B. M. 1953, *The Planet Jupiter: The Observer's Handbook* (Boston, MA: Faber and Faber)
- Perez-Hoyos, S., Sanchez-Lavega, A., Hueso, R., Garcia-Melendo, E., & Legarreta, J. 2009, *Icarus*, 203, 516
- Ragent, B., Colburn, D. S., Rages, K. A., Knight, T. C. D., Avrin, P., Orton, G. S., Yanamandra-Fisher, P. A., & Grams, G. W. 1998, *J. Geophys. Res.*, 103, 22891
- Rages, K. A., Hammel, H. B., & Friedson, A. J. 2004, *Icarus*, 172, 548
- Rages, K. A., Hammel, H. B., & Sromovsky, L. 2007, *Bull. Am. Astron. Soc.*, 39, 425
- Roos-Serote, M., Drossart, P., Encrenaz, T., Lellouch, E., Carlson, R. W., Baines, K. H., Kamp, L., Mehlman, R., Orton, G. S., Calcutt, S., Irwin, P., Taylor, F., & Weir, A. 1998, *J. Geophys. Res.*, 103, 23032
- Sánchez-Lavega, A. 1982, *Icarus*, 49, 1
- Sánchez-Lavega, A. 2010, *An Introduction to Planetary Atmospheres* (Boca Raton, FL: CRC)
- Sánchez-Lavega, A., Colas, F., Lecacheux, J., Laques, P., Parker, D., & Miyazaki, I. 1991, *Nature*, 353, 397
- Sánchez-Lavega, A., del Río-Gaztelurrutia, T., Hueso, R., Gómez-Forrellad, J. M., Sanz-Requena, J. F., Legarreta, J., García-Melendo, E., Colas, F., Lecacheux, J., Fletcher, L. N., Barrado-Navascués, D., Parker, D., & The International Outer Planet Watch Team 2011, *Nature*, 475, 71
- Seiff, A., Kirk, D. B., Knight, T. C. D., Young, R. E., Mihalov, J. D., Young, L. A., Milos, F. S., Schubert, G., Blanchard, R. C., & Atkinson, D., 1998, *J. Geophys. Res.*, 103(E10), 22857
- Simon-Miller, A. A., Conrath, B., Gierasch, P. J., & Beebe, R. F. 2000, *Icarus*, 145, 454
- Simon-Miller, A. A., Banfield, D., & Gierasch, P. J. 2001a, *Icarus*, 149, 94
- Simon-Miller, A. A., Banfield, D., & Gierasch, P. J. 2001b, *Icarus*, 154, 459
- Sromovsky, L. A., & Fry, P. M. 2002, *Icarus*, 157, 373
- Sromovsky, L. A., & Fry, P. M. 2005, *Icarus*, 179, 459
- Sromovsky, L. A., & Fry, P. M. 2010, *Icarus*, 210, 230
- Sromovsky, L. A., Revercomb, H. E., Krauss, R. J., & Suomi, V. E. 1983, *J. Geophys. Res.*, 88, 8650
- Sromovsky, L. A., Collard, A. D., Fry, P. M., Orton, G. S., Lemmon, M. T., Tomasko, M. G., & Freedman, R. S. 1998, *J. Geophys. Res.*, 103, 22929
- Sromovsky, L. A., Fry, P. M., Limaye, S. S., & Baines, K. H. 2003, *Icarus*, 163, 256
- Sromovsky, L. A., Fry, P. M., Hammel, H. B., de Pater, I., Rages, K. A., & Showalter, M. R. 2007, *Icarus*, 192, 558
- Strycker, P. D., Chanover, N. J., Simon-Miller, A. A., Banfield, D., & Gierasch, P. J. 2011, *Icarus*, 215, 552
- von Zahn, U., Hunten, D. M., & Lehmacher, G. 1998, *J. Geophys. Res.*, 103, 22815
- Weidenschilling, S. J., & Lewis, J. S. 1973, *Icarus*, 20, 465
- West, R. A., Strobel, D. F., & Tomasko, M. G. 1986, *Icarus*, 65, 161
- West, R. A., Baines, K. H., Friedson, A. J., Banfield, D., Ragent, B., & Taylor, F. W. 2004, in *Jupiter: The Planet, Satellites, and Magnetosphere*, ed. F. Bagenal et al. (Cambridge, UK: Cambridge University Press), 79–104
- Westphal, J. A., Baum, W. A., Ingersoll, A. P., Barnet, C. D., de Jong, E. M., Danielson, G. E., & Caldwell, J. 1992, *Icarus*, 98, 94
- Young, R. E. 2003, *New Astron. Rev.*, 47, 1
- Young, R. E., Smith, M. A., & Sobek, C. K. 1996, *Science*, 272, 837